CSIRO PUBLISHING

Australian Journal of Physics

Volume 50, 1997

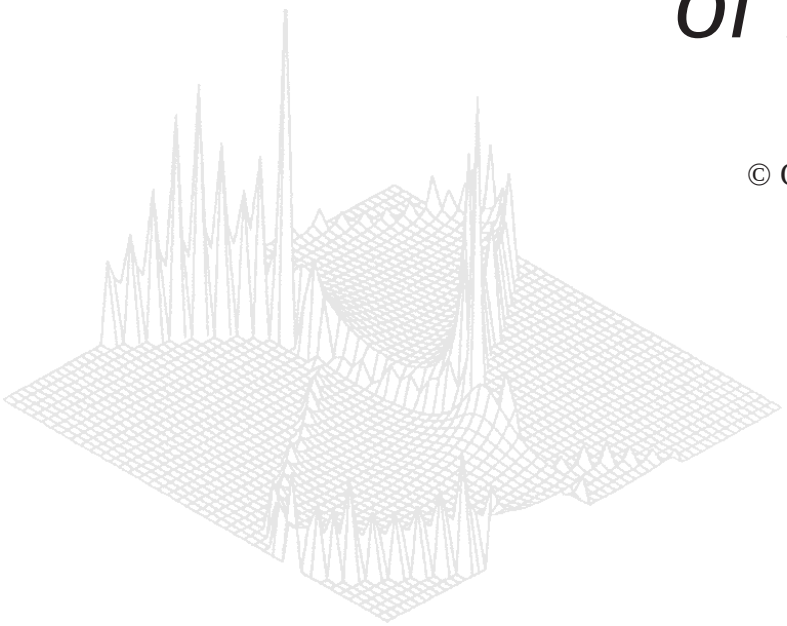

A journal for the publication of
original research in all branches of physics

www.publish.csiro.au/journals/ajp

All enquiries and manuscripts should be directed to
Australian Journal of Physics
CSIRO PUBLISHING
PO Box 1139 (150 Oxford St)
Collingwood Telephone: 61 3 9662 7626
Vic. 3066 Facsimile: 61 3 9662 7611
Australia Email: peter.robertson@publish.csiro.au

Published by **CSIRO** PUBLISHING
for CSIRO Australia and
the Australian Academy of Science

Aust. J. Phys., 1997, **50**, 281–308

Coherent Population Transfer among Three States: Full Algebraic Solutions and the Relevance of Non Adiabatic Processes to Transfer by Delayed Pulses

M. P. Fewell,[A] *B. W. Shore*[B] *and K. Bergmann*

Fachbereich Physik der Univeristät, Postfach 3049,
67653 Kaiserslautern, Germany.
[A] Permanent address: Department of Physics,
University of New England, Armidale, NSW 2351, Australia.
[B] Permanent address: Lawrence Livermore National Laboratory,
Livermore, CA 94550, USA.

Abstract

Ongoing work aimed at developing highly efficient methods of populating a chosen sublevel of an energy level highlights the need to understand off-resonant effects in coherent excitation. This motivated us to re-examine some aspects of the theory of coherent excitation in a three-state system with a view to obtaining algebraic expressions for off-resonant eigenvalues and eigenvectors. Earlier work gives simple closed-form expressions for the eigenvalues this system, expressions applying even when the system is not on two-photon resonance. We present here expressions of similar simplicity for the components of the normalised eigenvectors. The analytic properties of these components explain the observed sensitivity of the stimulated-Raman-adiabatic-passage process (STIRAP) to the condition of two-photon resonance. None of the eigenstates is 'trapped' or 'dark' unless the system is on two-photon resonance; off resonance, all states have nonzero projections on the unperturbed intermediate state. A simple argument shows that no dressed state can be adiabatically connected to both the unperturbed initial and final states when the system is off two-photon resonance. That is, adiabatic transfer from initial to final state requires that these be degenerate before and after the STIRAP pulse sequence, and this implies zero two-photon detuning. However, substantial transfer probabilities are observed experimentally for very small two-photon detunings. We show that such systems are characterised by very sharp avoided crossings of two eigenvalues, and that the observed population transfer can be understood as an effect of non adiabatic transitions occurring at the avoided crossings.

1. Introduction

The search for efficient ways of preparing atoms or molecules in a selected excited state is a major theme of atomic and molecular physics. There is particular current interest in accessing high vibrational levels efficiently and selectively, and in transferring population 'via' a decaying state without the detrimental effect of radiative loss. It has long been recognised that adiabatic procedures, in which an atom remains at all times in one eigenstate of a smoothly changing Hamiltonian, offer opportunities for complete population transfer in two-level (e.g. Hamadani *et al.* 1975; Avrillier *et al.* 1981; Adams *et al.* 1985) and three-level systems (Oreg *et al.* 1984, 1985; Carroll and Hioe 1986*a*, 1986*b*, 1987*a*, 1987*b*, 1988*a*, 1988*b*, 1989; Hioe 1987; Carroll 1989; Kuklinski *et al.* 1989). Implementation of this theoretical ideal in multilevel systems poses technical problems that have, in recent years, been successfully overcome with the use of a coherent pulsed

10.1071/PH96071 0004-9506/97/020281$10.00

excitation mechanism termed 'stimulated Raman adiabatic passage' (STIRAP) (Gaubatz *et al.* 1990; Schiemann *et al.* 1992). This method has been demonstrated on atoms (Rubahn *et al.* 1991; Broers *et al.* 1992) and molecules (Gaubatz *et al.* 1990; Dam *et al.* 1990; Schiemann *et al.* 1993; Halfmann and Bergmann 1996), and is being used as an experimental tool in crossed-beam reactive-scattering experiments (Ditmann *et al.* 1992; Külz *et al.* 1996), for spectroscopic studies (Süssmann *et al.* 1994) and in the context of atomic interferometry (Marte *et al.* 1991; Kasevich *et al.* 1991; Kasevich and Chu 1991, 1992; Lawall and Prentiss 1994; Goldner *et al.* 1994). Bergmann and Shore (1995) have recently reviewed STIRAP.

(1a) Overview of the STIRAP Process

The simplest STIRAP scheme involves three non degenerate states of an atom or molecule: the initial state, an intermediate state, and the target final state. Two overlapping pulses of coherent laser light induce the desired transition from initial state to final state. One laser pulse, the 'pump' pulse, couples the initial and intermediate states. The other, the 'Stokes' pulse, couples the intermediate and final states. Typically, the carrier frequencies of the laser light are near, but not necessarily equal to, the values corresponding to the bare-state resonances. The two carrier frequencies together must be tuned to two-photon resonance. Fig. 1 shows schematically the so-called lambda configuration, in which the intermediate state lies highest in energy. Detunings Δ_p from one-photon resonance and Δ_3 from two-photon resonance are indicated.

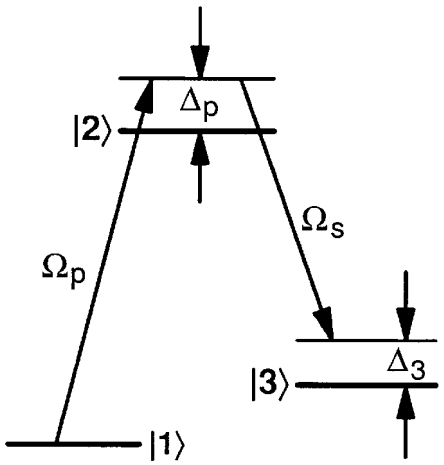

Fig. 1. Coupling scheme typical of a STIRAP experiment in the lambda configuration. The pump laser, with Rabi frequency Ω_p, has its carrier frequency ω_p detuned by Δ_p from resonance with the intermediate level $|2\rangle$. The Stokes laser has carrier frequency ω_s and Rabi frequency Ω_s. The two lasers are detuned by Δ_3 from two-photon resonance with the final level $|3\rangle$

The pulsed nature of the interaction between the laser light and the atoms or molecules can be produced either by causing the particles to traverse overlapping continuous-wave laser beams or by illuminating essentially stationary particles with pulsed lasers. The crucial distinguishing characteristic of STIRAP, in contrast to conventional stimulated Raman excitation, is that the overlapping pulses must be ordered counter-intuitively; that is, the atom or molecule must encounter the Stokes pulse first.

If two-photon resonance is maintained, and if the pulses meet certain coherence and adiabaticity conditions (Gaubatz *et al.* 1990; He *et al.* 1990; Kuhn *et al.* 1992; Bergmann and Shore 1995), then complete population transfer occurs. During the transfer, no population ever appears in the intermediate state. Thus, the possibility of spontaneous decay of the intermediate state cannot reduce the efficiency of the transfer, even when the duration of the light pulses is much longer than the lifetime of the intermediate state. This effect is closely related to the phenomenon of the dark resonance, which was perhaps the first of the coherently driven three-state phenomena to be recognised (Arimondo and Orriols 1976; Alzetta *et al.* 1979; Orriols 1979; Narducci *et al.* 1990; Manka *et al.* 1991).

The concept of the original three-state STIRAP scheme has been adapted to a variety of more elaborate systems (Dam *et al.* 1990; Shore *et al.* 1991, 1992; Oreg *et al.* 1992), involving interaction with the continuum (Carroll and Hioe 1992, 1993, 1995; Nakajima *et al.* 1994) or additional quantum states (Shore *et al.* 1995; Martin *et al.* 1995, 1996) to describe real atoms and molecules better. The inclusion of additional levels, such as magnetic sublevels, introduces new features: there may be more than one dark intermediate level and the target level may contain degenerate sublevels. Recent theoretical (Shore *et al.* 1995; Martin *et al.* 1995) and experimental (Martin 1995; Martin *et al.* 1996) studies have revealed interesting properties of the STIRAP-type coherent population-transfer process in multilevel systems where the participating quantum states are degenerate or nearly so. In particular, this work has shown how to use STIRAP for transfer of population into a selected magnetic sublevel, that is, to produce orientation of electronic or rotational angular momentum. The selectivity is provided merely by changing the carrier frequency of one laser. In this situation, coupling occurs to more than one of the distinct non degenerate final states; for, although two-photon resonance occurs with only one of the manifold of final levels at any time, coupling to adjacent magnetic sublevels may be nonzero as well.

Both theoretical modelling and experimental observation have shown that, although STIRAP is relatively insensitive to single-photon resonance, the efficiency of population transfer relies critically on the occurrence of two-photon resonance. The two-photon linewidth in STIRAP is very narrow. Thermally induced Doppler shifts, such as are encountered in a gas cell or in other than highly collimated particle beams, are one example of effects preventing the establishment of two-photon resonance for all atoms or molecules exposed to the laser light. On two-photon resonance, the efficiency of transfer is insensitive to details of the laser pulses such as pulse shape or total pulse energy, provided that these are such as to meet the adiabaticity conditions. The only critical characteristic of the pulse sequence is the separation between the two pulses; this should be about one quarter of their width.

The present work was motivated by a desire to understand further how the transfer process is influenced by detuning from two-photon resonance and the relevance of adiabatic *versus* non adiabatic processes. These effects are most readily explored in the simplest STIRAP system: the three-state system. Our algebraic analysis shows that the relevance of non adiabatic processes has been underestimated in recent discussions (Gaubatz *et al.* 1990; He *et al.* 1990; Kuhn *et al.* 1992; Bergmann and Shore 1995), at least partly because there has not been a full appreciation of the importance of non adiabatic transitions when slightly

detuned from two-photon resonance. Some numerical studies of non adiabatic processes in STIRAP have also been presented (Danileiko *et al.* 1994).

(1b) Adiabatic and Non Adiabatic Evolution

The essential ingredients of STIRAP are the counter-intuitive order of the laser pulses and the related evolution of the eigenstates of the time-dependent Hamiltonian. When coherent radiation is present, the Hamiltonian of the system as a whole includes both atomic-excitation energy and field-interaction energy; its eigenstates are the dressed states. As the Hamiltonian changes with varying laser-light intensity, the instantaneous dressed states change their composition. We use the term 'adiabatic state' to refer to such time-varying dressed states. For excitation on two-photon resonance, an adiabatic state connects the initial and final bare-atom states. This adiabatic state, called the STIRAP state, is also orthogonal to the intermediate state at all times during the pulse sequence. The counter-intuitive order of the laser pulses ensures that the system enters the STIRAP state (Gaubatz *et al.* 1990). If the system remains in the STIRAP state at all times, then the intermediate state is never populated during the population transfer, though its presence is necessary to define the orientation of the STIRAP state in Hilbert space.

The STIRAP state can be an effective conduit for population transfer only if it remains populated during the pulse sequence. This introduces the notion of adiabatic evolution of the system. During an *adiabatic* process, the environment of the atom or molecule changes sufficiently slowly that the particle remains at all times in one adiabatic state. A non adiabatic (or *diabatic*) process involves transitions between the adiabatic states. The original concept of STIRAP involved the system entering the STIRAP state and remaining in it as it evolves from the initial unperturbed state through a superposition of atomic states to the final target state.

In principle, the construction of instantaneous dressed states poses no great numerical challenge even in multilevel systems: one need only diagonalise a finite matrix by means of a similarity transform. The columns of the transformation matrix, suitably ordered and normalised, provide the desired adiabatic states. Nevertheless, it is instructive to obtain analytic expressions for these components, when possible, in order to identify key components at early and late times in the pulse sequence, and so to identify conditions under which the desired population transfer will occur. Analytic expressions are also useful in designing an experiment, in that they may lead to estimates of one-photon and two-photon line widths.

Section 2 presents the required analytic expressions and Section 3 uses them to explore the time development of the eigenvalues and eigenvectors during a typical STIRAP pulse sequence. This is done for a variety of detunings, including examples of completely off-resonance cases. A simple argument shows that, when the system is off two-photon resonance, none of the adiabatic states connects the initial state at the start of the STIRAP pulse sequence to the final state at the end. Such a connection requires that the initial and final states be degenerate, and this implies two-photon resonance.

It is emphasised in Section 3*d* that strictly adiabatic population transfer occurs only when the laser carrier frequencies are tuned exactly to two-photon resonance.

In any real experiment this resonance condition cannot be established for all particles; diabatic processes are necessarily involved. From the considerations presented in Section 3*d*, it seems that such diabatic processes can be efficient if the two-photon detuning is small. Danileiko *et al.* (1994) have presented numerical studies of diabatic transition probabilities in STIRAP, calculated using Landau–Zener formalism. Off two-photon resonance, all dressed states acquire nonzero components of the intermediate state. The extent of this is discussed in Section 3*d*.

(1c) Relationship to Previous Work

Treatment of coherent excitation in a three-state system requires solutions to a cubic eigenvalue equation. Algebraic expressions for the roots of a cubic equation are well known (e.g. Abramowitz and Stegun 1973), and these can be reduced to a simple form in this case. This has been presented in other contexts by Radmore and Knight (1982) and Wilson and Hahn (1982). Nevertheless, it does not seem to be widely recognised that the eigenvalues of a three-state system have a simple form when the system is off two-photon resonance (e.g. comments by Sarkisyan and Ter-Mikaelyan 1978; Agarwal *et al.* 1979; Chang and Schlier 1980; Kuz'min and Sazonov 1980; Kuz'min 1981; Kancheva *et al.* 1981; Senitzky 1982; Carroll and Hioe 1987*a*, 1988*a*; Coulston and Bergmann 1992; Kuhn *et al.* 1992). Some previous treatments of the eigenvalue problem used expansions, assuming that the two-photon detuning is small (Agarwal *et al.* 1979; Chang and Schlier 1980).

Section 2*b* presents full solutions to the eigenvalue problem in a form appropriate for the present purpose. Given the eigenvalues of a matrix, elementary procedures can, in principle, provide unnormalised eigenvectors. Formal expressions for the normalisation factors follow directly (Radmore and Knight 1982; Radmore 1982). However, complications arise when a normalisation factor goes to zero or when eigenvalues are degenerate. In any chosen formulation, these singularities are likely to occur at some time during a STIRAP pulse sequence. Complete analysis of STIRAP, with the unambiguous pairing of a given eigenvector to its eigenvalue, requires a robust and explicit normalisation procedure.

We propose such a procedure in Section 2*c* by exploiting the formal equivalence between rotations of three-vectors and the time evolution of the system's three dressed states under the influence of a STIRAP pulse sequence. This method reduces the eigenvector problem to one of determining the orientation of a triad of automatically orthonormal vectors in a Hilbert space. Relatively simple expressions for the normalised components of the eigenvectors result. We show explicitly that, when the system is off two-photon resonance, none of the dressed states is orthogonal to the intermediate state for all values of the Rabi frequencies. This result has been noted previously (Radmore and Knight 1982; Radmore 1982). Here we use it to explore the dependence of STIRAP on two-photon resonance.

The only previous analytical treatment of off-two-photon-resonance effects in STIRAP was performed using the 'interaction picture' (Coulston and Bergmann 1992; Kuhn *et al.* 1992). This formalism gives simple expressions for both eigenvalues and eigenvectors. However, off two-photon resonance, the interaction-picture eigenvectors have oscillatory components, and this complicates the interpretation.

2. General Three-state Excitation

(2a) The Hamiltonian

The initial state $|1\rangle$, intermediate state $|2\rangle$ and final state $|3\rangle$ have energies E_1, E_2 and E_3 respectively in the unperturbed, or bare-atom, basis. We set E_1 to zero. The pump and Stokes fields, with carrier frequencies ω_p and ω_s respectively, cause a coherent mixing of basis states, described by the usual rotating-wave-approximation Hamiltonian (e.g. Shore 1990)

$$H = \frac{\hbar}{2}\begin{pmatrix} 0 & \Omega_\mathrm{p} & 0 \\ \Omega_\mathrm{p} & 2\Delta_\mathrm{p} & \Omega_\mathrm{s} \\ 0 & \Omega_\mathrm{s} & 2\Delta_3 \end{pmatrix} . \tag{1}$$

We have chosen phases so that the Hamiltonian is real. In equation (1), Ω_p and Ω_s are the Rabi frequencies describing the interaction with the pump and Stokes fields respectively and Δ_p, Δ_3 are detunings from resonance. These are defined by

$$\begin{aligned} \Delta_\mathrm{p} &= \omega_\mathrm{p} - E_2/\hbar \,, \\ \Delta_\mathrm{s} &= \omega_\mathrm{p} - |E_2 - E_3|/\hbar \,, \\ \Delta_3 &= \Delta_\mathrm{p} - \Delta_\mathrm{s} \,. \end{aligned} \tag{2}$$

[We are considering here the lambda configuration depicted in Fig. 1, in which E_2 is greater than both E_1 and E_3. In the ladder configuration, where $E_1 < E_2 < E_3$, the last line of equation (2) reads: $\Delta_3 = \Delta_\mathrm{p} + \Delta_\mathrm{s}$.] The Hamiltonian of equation (1) differs from that of Gaubatz *et al.* (1990) and He *et al.* (1990) by a shift in the origin of the energy scale.

In STIRAP, the Rabi frequencies are time-varying and the detunings are fixed. Two-photon resonance corresponds to $\Delta_3 = 0$. For convenience, we refer to the condition $\Delta_\mathrm{p} = \Delta_3 = 0$ as *one-photon resonance*. The term *pump resonance* refers to $\Delta_\mathrm{p} = 0$ and the condition $\Delta_\mathrm{s} = 0$ is called *Stokes resonance*.

(2b) Eigenvalues

The eigenvalues of H are the roots of the secular equation which, in this case, is the cubic equation

$$\omega^3 - 2(\Delta_\mathrm{p} + \Delta_3)\omega^2 - (\Omega_\mathrm{p}^2 + \Omega_\mathrm{s}^2 - 4\Delta_\mathrm{p}\Delta_3)\omega + 2\Omega_\mathrm{p}^2\Delta_3 = 0 \,. \tag{3}$$

The general solutions of this equation are

$$\begin{aligned} \omega^0 &= \tfrac{2}{3}\left(\Delta_\mathrm{p} + \Delta_3 + \tilde{\Omega}\cos\frac{\zeta}{3}\right) , \\ \omega^+ &= \tfrac{2}{3}\left(\Delta_\mathrm{p} + \Delta_3 + \tilde{\Omega}\cos\frac{2\pi - \zeta}{3}\right) , \\ \omega^- &= \tfrac{2}{3}\left(\Delta_\mathrm{p} + \Delta_3 + \tilde{\Omega}\cos\frac{2\pi + \zeta}{3}\right) , \end{aligned} \tag{4}$$

where the auxiliary variables $\tilde{\Omega}$ and ζ are defined by

$$\tilde{\Omega} = [3(\Omega_{\rm p}^2 + \Omega_{\rm s}^2) + 4(\Delta_{\rm p}^2 - \Delta_{\rm p}\Delta_3 + \Delta_3^2)]^{\frac{1}{2}}\,, \tag{5}$$

$$\zeta = 2\pi - \arccos\frac{[9(\Omega_{\rm p}^2 + \Omega_{\rm s}^2) - 4(2\Delta_{\rm p} - \Delta_3)(2\Delta_3 - \Delta_{\rm p})](\Delta_{\rm p} + \Delta_3) - 27\Omega_{\rm p}^2\Delta_3}{\tilde{\Omega}^3}\,. \tag{6}$$

That equations (4–6) give solutions of equation (3) can be verified by direct substitution. The superscripts labelling the roots of equations (4) have been chosen to conform with standard labels in the literature of STIRAP (Kuklinski *et al.* 1989; Gaubatz *et al.* 1990). Details are given in Appendix A. The labelling depends on the appearance of the 2π in the definition of ζ and on the range adopted for the inverse cosine function. We choose the range such that $\pi < \zeta < 2\pi$. Since it then follows that

$$\begin{aligned} \left|\cos\left(\frac{\zeta}{3}\right)\right| &\leq \tfrac{1}{2}, \\ \tfrac{1}{2} \leq \left|\cos\left(\frac{2\pi - \zeta}{3}\right)\right| &\leq 1\,, \\ -1 \leq \left|\cos\left(\frac{2\pi + \zeta}{3}\right)\right| &\leq -\tfrac{1}{2}\,, \end{aligned} \tag{7}$$

equations (4) show that the eigenvalues are always ordered,

$$\omega^- \leq \omega^0 \leq \omega^+ \tag{8}$$

for all values of Rabi frequencies and detunings. This result is useful for understanding the behaviour of the three-state system undergoing a STIRAP pulse sequence.

(2c) Eigenvectors and Mixing Angles

The simplest procedure for constructing an eigenvector, given an eigenvalue, is to set one component of the eigenvector to unity, so that the eigenvector equation becomes a set of inhomogeneous equations. Application of, say, Kramer's rule then provides analytic expressions for each of the eigenvector components in terms of matrix elements and eigenvalues. Apart from the algebraic complexity of the resulting normalisation factors, this procedure is unsatisfactory when the eigenvector component chosen to be unity is, in fact, zero; for then the normalisation factor is infinite. Any choice of eigenvector component will produce this effect in some circumstances, and this can cause a problem in the construction of an algebraic description valid for the whole of a STIRAP pulse sequence.

To avoid difficulties associated with direct normalisation and to obtain expressions valid for all values of the parameters, we instead exploit the formal correspondence between three-dimensional Hilbert space and ordinary three-space. On this view, the eigenvectors are obtained by rotating the triad of Cartesian basis vectors

$$|1\rangle = \begin{pmatrix} 1 \\ 0 \\ 0 \end{pmatrix}, \quad |2\rangle = \begin{pmatrix} 0 \\ 1 \\ 0 \end{pmatrix}, \quad |3\rangle = \begin{pmatrix} 0 \\ 0 \\ 1 \end{pmatrix}. \tag{9}$$

This produces a triad of automatically normalised mutually orthogonal real vectors as the dressed states. The time-dependent components of these rotated vectors are the probability amplitudes for population transfer.

General rotations of a three-vector can be described by the three-dimensional rotation matrix $\mathsf{D}(\alpha, \beta, \gamma)$, where α, β, γ are Euler angles. We start with the definition of Euler angles given in Zare (1988). To relate the resulting expressions to the two-photon-resonance expressions of Gaubatz *et al.* (1990), we identify $|\mathbf{a}^0\rangle$ with a rotated state $|\mathbf{1}\rangle$, $|\mathbf{a}^-\rangle$ with a rotated state $|\mathbf{3}\rangle$ and we introduce the left-handed mixing angles

$$\Phi = -\alpha, \;\; \Theta = -\beta, \quad \phi = -\gamma. \tag{10}$$

This leads to the following parametrisation for the dressed states:

$$\begin{aligned} |\alpha^0\rangle = {} & \cos\Theta|\mathbf{1}\rangle + \sin\Phi\sin\Theta|\mathbf{2}\rangle - \cos\Phi\sin\Theta|\mathbf{3}\rangle, \\ |\mathbf{a}^+\rangle = {} & \sin\Theta\sin\phi|\mathbf{1}\rangle - (\sin\Phi\cos\Theta\sin\phi - \cos\Phi\cos\phi)|\mathbf{2}\rangle \\ & + (\cos\Phi\cos\Theta\sin\phi + \sin\Phi\cos\phi)|\mathbf{3}\rangle, \\ |\mathbf{a}^-\rangle = {} & \sin\Theta\cos\phi|\mathbf{1}\rangle - (\sin\Phi\cos\Theta\cos\phi + \cos\Phi\sin\phi)|\mathbf{2}\rangle \\ & + (\cos\Phi\cos\Theta\cos\phi - \sin\Phi\sin\phi)|\mathbf{3}\rangle. \end{aligned} \tag{11}$$

The equations for two-photon resonance (Gaubatz *et al.* 1990) are recovered by setting Φ to zero.

In these terms, the objective of complete population transfer corresponds to rotating a dressed-state vector from $|\mathbf{1}\rangle$ to $|\mathbf{3}\rangle$. In the usual picture of STIRAP, which assumes two-photon resonance, the transfer involves the variation of the mixing angle Θ from zero to $\pi/2$, while maintaining Φ at zero. This is effectively a rotation of the triad about the direction corresponding to state $|\mathbf{2}\rangle$. When two-photon detuning is present, it is no longer adequate to visualise the process as a simple rotation about the direction of state $|\mathbf{2}\rangle$.

(2d) Ranges of the Mixing Angles

The set of Euler angles is in two-to-one correspondence with the set of all possible three-dimensional rotations (e.g. Messiah 1962). Thus, the range of Θ can be restricted to $0 \leq \Theta \leq \pi$ without loss of generality. In addition to this, the overall phase of each state vector is arbitrary. We follow the phase convention of Gaubatz *et al.* (1990), requiring that the components of basis state $|\mathbf{1}\rangle$ is never negative. Equations (11) show that this combination of choices restricts both Θ and ϕ to the first quadrant:

$$0 < \Theta < \pi/2, \quad 0 < \phi < \pi/2\,. \tag{12}$$

There is no *a priori* limit on the range of Φ. However, the nature of the problem is such that Φ always lies in the range

$$-\pi/2 < \Phi < \pi/2\,. \tag{13}$$

This is shown in Appendix E.

(2e) Expressions for the Mixing Angles

Equations (11) define parametrisations of the eigenvectors $|\mathbf{a}^i\rangle$ in terms of mixing angles. Expressions for the mixing angles in terms of detunings and Rabi frequencies can be obtained by matching the components of an eigenvector with solutions to the eigenvector equations. The results for Θ and Φ are

$$\Theta = \begin{cases} \pi/2 & \text{if } \Omega_\mathrm{s} = 0 \text{ and either} \\ & \Delta_3 = 0 \text{ or } \Delta_3 = \Delta_\mathrm{p} \\ \arctan\left|\dfrac{\Omega_\mathrm{p}[(\omega^0 - 2\Delta_3)^2 + \Omega_\mathrm{s}^2]^{1/2}}{(\omega^0 - 2\Delta_\mathrm{p})(\omega^0 - 2\Delta_3) - \Omega_\mathrm{s}^2}\right|, & \text{otherwise} \end{cases} \tag{14}$$

and

$$\tan\Phi = \begin{cases} 0 & \text{if } \Theta = 0 \\ (2\Delta_3 - \omega^0)/\Omega_\mathrm{s}, & \text{otherwise}\,. \end{cases} \tag{15}$$

These are derived in Appendix C.

It is not possible to find one expression for ϕ that is valid for all values of the parameters; different expressions must be used in different cases. Appendix D contains a detailed discussion, leading to the scheme set out in Table 1. This scheme is rather complicated, but it should be recognised that there are many special cases in which a singularity may occur. Table 1 covers these with just eight expressions.

(2f) Two-photon Resonance

On two-photon resonance, $\Delta_3 = 0$ and equation (3) is easy to solve, giving

$$\omega^0 = 0\,,$$

$$\omega^\pm = \Delta_\mathrm{p} \pm (\Omega_\mathrm{p}^2 + \Omega_\mathrm{s}^2 + \Delta_\mathrm{p}^2)^{\frac{1}{2}}\,. \tag{16}$$

The reduction of equations (4–6) to equations (16) by setting $\Delta_3 = 0$ is not straightforward; this is discussed in Appendix B. Equation (16) differs from the corresponding expression of Gaubatz *et al.* (1990) because of the different choice of the zero of the energy scale (see Section 2*a*).

Table 1. Method of calculating the angle ϕ

Conditions on angles	Conditions on detunings	$\tan\phi^{\mathrm{A}}$
$\Theta \le \pi/20$	$\Delta_3 \le 0 < \Delta_\mathrm{p}$ or $\Delta_3 > 0$ and $\Delta_\mathrm{p} = 0$	$\left\lvert \dfrac{X^+ \sin\Phi - \Omega_\mathrm{s}\cos\Phi}{(\Omega_\mathrm{s}\sin\Phi + X^+\cos\Phi)\cos\Theta} \right\rvert$
	otherwise	$\left\lvert \dfrac{(\Omega_\mathrm{s}\sin\Phi + X^-\cos\Phi)\cos\Theta}{X^-\sin\Phi - \Omega_\mathrm{s}\cos\Phi} \right\rvert$
$\Theta > \pi/20$ and $\lvert\Phi\rvert \le \pi/20$	$\Delta_\mathrm{p} \le \Delta_3 < 0$ or $\Delta_3 = 0$ and $\Delta_\mathrm{p} > 0$	$\left\lvert \dfrac{Y^+\cos\Phi}{\Omega_\mathrm{p}X^+\sin\Theta - Y^+\sin\Phi\cos\Theta} \right\rvert$
	otherwise	$\left\lvert \dfrac{\Omega_\mathrm{p}X^-\sin\Theta + Y^-\sin\Phi\cos\Theta}{Y^-\cos\Phi} \right\rvert$
Otherwise	$0 \le \Delta_\mathrm{p} < \Delta_3$	$\left\lvert \dfrac{\Omega_\mathrm{p}\Omega_\mathrm{s}\sin\Phi}{\Omega_\mathrm{p}\Omega_\mathrm{s}\cos\Phi\cos\Theta + Z^+\sin\Theta} \right\rvert$
	$\Delta_3 < 0$ and $\Delta_\mathrm{p} = 0$	$\left\lvert \dfrac{\Omega_\mathrm{p}\Omega_\mathrm{s}\cos\Phi\cos\Theta + Z^-\sin\Theta}{\Omega_\mathrm{p}\Omega_\mathrm{s}\sin\Phi} \right\rvert$
	$\Delta_3 > 0$ and either $\Delta_\mathrm{p} < 0$ or $\Delta_\mathrm{p} = \Delta_3$	$\left\lvert \dfrac{\Omega_\mathrm{p}\Omega_\mathrm{s}\sin\Theta + Y^-\cos\Phi\cos\Theta}{Y^-\sin\Phi} \right\rvert$
	otherwise	$\left\lvert \dfrac{Y^+\sin\Phi}{\Omega_\mathrm{p}\Omega_\mathrm{s}\sin\Theta + Y^+\cos\Phi\cos\Theta} \right\rvert$

[A] $X^i = \omega^i - 2\Delta_3$, $\quad Y^i = \Omega_\mathrm{s}^2 - (\omega^\mathrm{i} - 2\Delta_3)(\omega^i - 2\Delta_\mathrm{p})$, $\quad Z^i = \Omega_\mathrm{p}^2 - \omega^i(\omega^i - 2\Delta_\mathrm{p})$.

Since both Δ_3 and ω^0 are zero on two-photon resonance, equation (14) gives directly, in this case,

$$\tan\Theta = \Omega_\mathrm{p}/\Omega_\mathrm{s}\,, \tag{17}$$

in agreement with Gaubatz *et al.* (1990). Equation (15) then gives $\Phi = 0$, as foreshadowed in Section 2*c*. Suitable expressions for $\tan\phi$ are therefore the top two entries in Table 1 when Ω_s is much smaller than Ω_s, and the third and fourth entries otherwise. Insertion of equations (16) and (17) into the top four expressions in Table 1 leads to the same result:

$$\tan\phi = \frac{(\Omega_\mathrm{p}^2 + \Omega_\mathrm{s}^2)^{\frac{1}{2}}}{(\Omega_\mathrm{p}^2 + \Omega_\mathrm{s}^2 + \Delta_\mathrm{p}^2)^{\frac{1}{2}} + \Delta_\mathrm{p}}\,. \tag{18}$$

This agrees with the expression of Gaubatz *et al.* (1990) when the different location of the zero of energy is taken into account.

3. Results with the STIRAP Pulse Sequence

We now use the algebraic results of Section 2 to examine the evolution of the eigenvalues and eigenvectors under the influence of a sequence of laser pulses

typical of STIRAP. Our objective is to identify conditions that lead to substantial likelihood of the desired population transfer.

(3a) The Pulse Sequence

In STIRAP, the Rabi frequencies are time-varying in such a way that the pump frequency $\Omega_{\rm p}(t)$ is zero early in the pulse sequence and the Stokes frequency $\Omega_{\rm s}(t)$ is zero late in the sequence. A convenient representation of such a pulse sequence is

$$\Omega_{\rm p}(t) = \Omega_0\, p(t-\tau)\,,\ \ \Omega_{\rm s}(t) = \Omega_0\, p(t)\,, \tag{19}$$

where $p(t)$ is a pulse envelope of unit maximum value. A useful choice, giving a pulse shape reminiscent of a Gaussian but limited to a finite duration, is (Shore *et al.* 1991, 1992; Oreg *et al.* 1992)

$$p(t) = \begin{cases} \sin^4(\pi t/T), & 0 < \mathrm{t} < \mathrm{T} \\ 0, & \text{otherwise}\,. \end{cases} \tag{20}$$

To produce optimal overlap, we choose $\tau = 0\cdot 2T$ in all figures below. Fig. 2 shows the resulting pulse sequence.

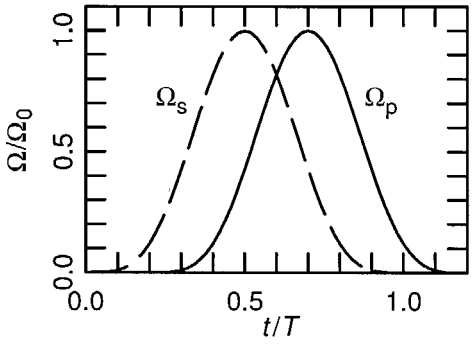

Fig. 2. Time development of Rabi frequency in a typical STIRAP sequence of laser pulses. The Rabi frequency of the pump pulse ($\Omega_{\rm p}$) is shown by the full curve and that of the Stokes pulse ($\Omega_{\rm s}$) by the broken curve. Each pulse has duration of T and a maximum Rabi frequency of Ω_0. The Stokes pulse leads the pump pulse by $\tau = 0\cdot 2T$.

Insofar as adiabatic passage occurs, the results are independent of T and of the amplitude Ω_0. The latter provides a convenient energy scale. The results of experiment and computer simulations suggest that there is no loss of significant generality either in the choice of this pulse shape (rather than, say, a Gaussian) or in choosing the pump and Stokes pulses to have the same amplitude. This reflects the robustness of STIRAP against variation in the details of the pulses.

(3b) Adiabatic Eigenvalues

Plots of adiabatic eigenvalues offer guides for predicting population transfer: if the evolution is adiabatic, then the system tracks the course of an eigenvalue. Fig. 3 shows, for a range of values of detunings $\Delta_{\rm p}$ and Δ_3, plots of the time development of the eigenvalues ω^i (equations 4) as the system encounters the STIRAP pulse sequence of Fig. 2. The panels are ordered with increasing Δ_3 to the right and decreasing $\Delta_{\rm p}$ down. Fig. 3*g* is the case of one-photon resonance.

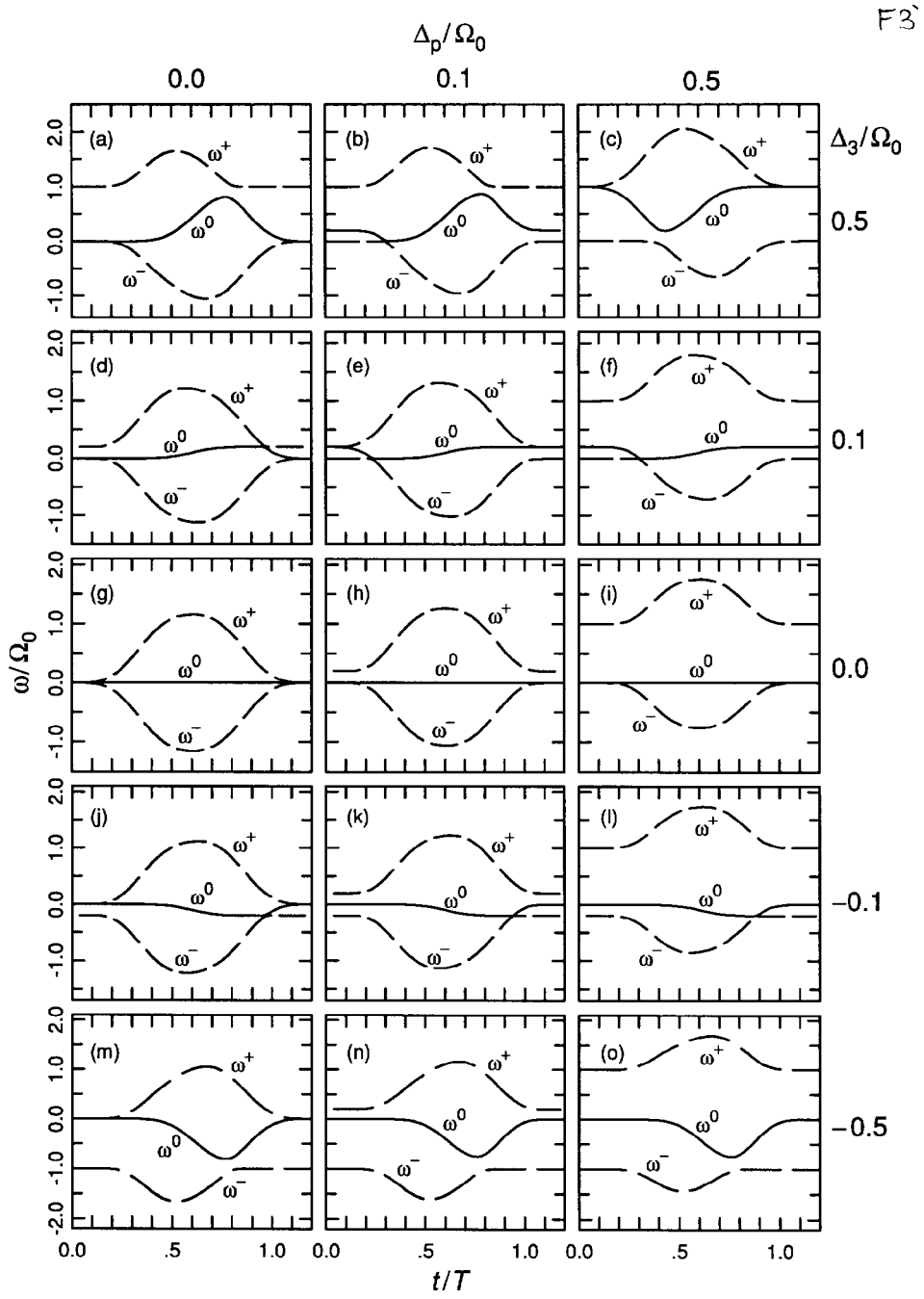

Fig. 3. Time evolution of the eigenvalues ω of a three-state system encountering the STIRAP pulse sequence shown in Fig. 2. The panels show results for various detunings, as indicated at the top and to the right. The full curves show values of ω^0 and the broken curves values of ω^+ and ω^-. All eigenvalues and detunings are normalised to the peak Rabi frequency Ω_0. Special cases are: *g* one-photon resonance, *g–i* two-photon resonance, *a, d, g, j, m* pump resonance, and *c, e, g* Stokes resonance.

The central row of panels (Figs 3*g*–3*i*) shows cases of two-photon resonance. The left column (Figs 3*a*, 3*d*, 3*g*, 3*j*, 3*m*) contains cases of pump resonance ($\Delta_\mathrm{p} = 0$) and Figs 3*c*, 3*e*, 3*g* cases of Stokes resonance ($\Delta_\mathrm{p} = \Delta_3$, that is $\Delta_\mathrm{s} = 0$). Results for negative values of Δ_p can be obtained by a symmetry operation: to obtain the plot for $-\Delta_\mathrm{p}$, Δ_3 turn the plot for $\Delta_p, -\Delta_3$ upside down and exchange the labels ω^+ and ω^-.

By definition, the system starts in state $|\mathbf{1}\rangle$; the energy of this state serves as the zero point. The energies of the unperturbed states are 0, $\hbar\Delta_\mathrm{p}$ and $\hbar\Delta_3$. These equal the initial and final dressed eigenvalues. When $\Delta_\mathrm{p} \neq \Delta_3$ and neither detuning is zero, the asymptotic eigenvalues of the dressed states are distinct. If a system with these detunings evolves adiabatically from the outset, then it populates the dressed state with zero asymptotic eigenvalue. Which dressed state this is depends on the ordering of Δ_p and Δ_3 with respect to zero. Continued adiabatic evolution then results in the system returning to state $|\mathbf{1}\rangle$, the initial state. The final state, which has an asymptotic eigenvalue of Δ_3, is not adiabatically accessible in this case.

This argument shows that adiabatic transfer of population from state $|\mathbf{1}\rangle$ to state $|\mathbf{3}\rangle$ can only occur if these two states are degenerate, and this implies $\Delta_3 = 0$, that is, two-photon resonance. On the other hand, many of the panels of Fig. 3 show sharp avoided crossings, raising the possibility of the desired transfer of population occurring by diabatic transitions near these crossings. This possibility is considered case by case in the next section.

(3c) Adiabatic and Diabatic Population Transfer

Triad-orientation Diagrams

The eigenvectors of a three-state system span a space isomorphic with real 3-space. This permits a pictorial representation of their evolution during a typical STIRAP pulse sequence. The evolution is modelled by the motion of an orthonormal triad of vectors relative to the directions of the unperturbed states $|\mathbf{1}\rangle$, $|\mathbf{2}\rangle$ and $|\mathbf{3}\rangle$. The required orientation angles are just the Euler angles introduced in Section 2*c*.

Fig. 4 consists of such a pictorial representation for the simplest case: that of one-photon resonance. Each panel of Fig. 4 shows the orientation of the triad of dressed states at the indicated times during the pulse sequence. For convenience, the Rabi frequencies at the times chosen are listed in Table 2. For the case shown in Fig. 4, eigenvector $|\mathbf{a}^0\rangle$ initially corresponds with state $|\mathbf{1}\rangle$. Thus, $|\mathbf{a}^0\rangle$ is the system state vector if adiabatic following occurs. To aid in the visualisation of the rotation, broken lines indicate the components of $|\mathbf{a}^+\rangle$ and $|\mathbf{a}^-\rangle$, where practicable.

The remainder of this section explores the details in Fig. 4 and in other more general cases to assess the possibilities for a transfer of population from state $|\mathbf{1}\rangle$ to state $|\mathbf{3}\rangle$.

Standard STIRAP

In its usual form, the concept of STIRAP assumes two-photon resonance. Fig. 4 shows the special case of one-photon resonance; the other cases are shown in Figs 5 and 6. Fig. 5 pertains to a system with positive pump detuning and

Fig. 6 to negative pump detuning. The times chosen are the same as in Fig. 4. Figs 3*g*–3*i* are the relevant eigenvalue plots. On one-photon resonance (Fig. 3*g*), the eigenvalues are three-fold degenerate before and after the pulse sequence. At nonzero pump detunings, one of the unperturbed eigenenergies is distinct, but there remains a two-fold degeneracy: between ω^0 and ω^- if Δ_p is positive and between ω^0 and ω^+ when Δ_3 is negative.

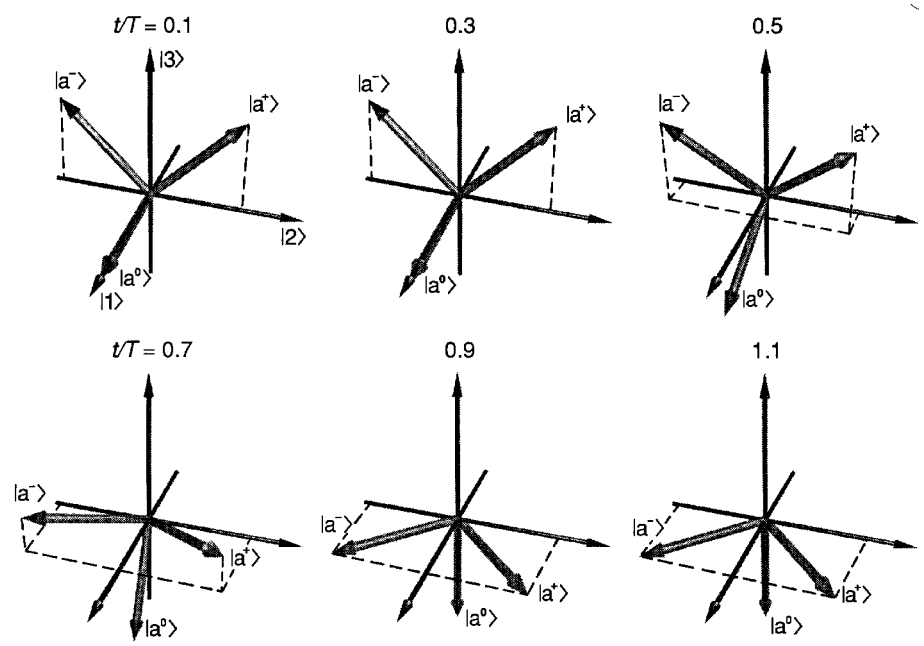

Fig. 4. Orientations of the triad of vectors representing the dressed states $|\mathbf{a}^0\rangle$, $|\mathbf{a}^+\rangle$ and $|\mathbf{a}^-\rangle$ of a three-state system on one-photon resonance at six times during the pulse sequence of Fig. 2, as indicated. The unperturbed states are shown as $|1\rangle$ (initial state), $|2\rangle$ (intermediate state) and $|3\rangle$ (final state). The eigenstate $|\mathbf{a}^0\rangle$, which corresponds with state $|1\rangle$ initially, is the state vector of the system if adiabatic following occurs. Broken lines indicate the components of $|\mathbf{a}^+\rangle$ and $|\mathbf{a}^-\rangle$, where practicable.

Table 2. Values of the Rabi frequencies Ω_p and Ω_s at times t used in Figs 4–7 and 9–12

t/T	Ω_p/Ω_0	Ω_s/Ω_0
0·1	0·000	0·009
0·3	0·009	0·428
0·5	0·428	1·000
0·7	1·000	0·428
0·9	0·428	0·009
1·1	0·009	0·000

The motions of the eigenvectors illustrated in Figs 4–6 show several points of similarity. In the first part of the STIRAP pulse sequence, the pump Rabi frequency Ω_p is zero, and so Θ is zero (equation 17). The first panels of Figs 4–6 show the situation at this time, when the eigenstate $|\mathbf{a}^0\rangle$ coincides with the

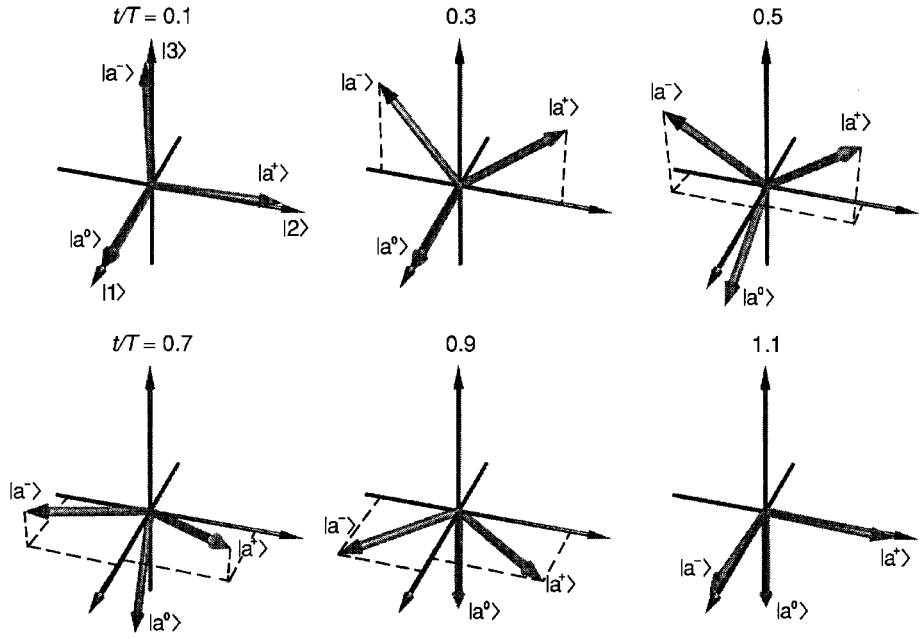

Fig. 5. As in Fig. 4, but for two-photon resonance with positive pump detuning ($\Delta_p = 0 \cdot 1\Omega_0$).

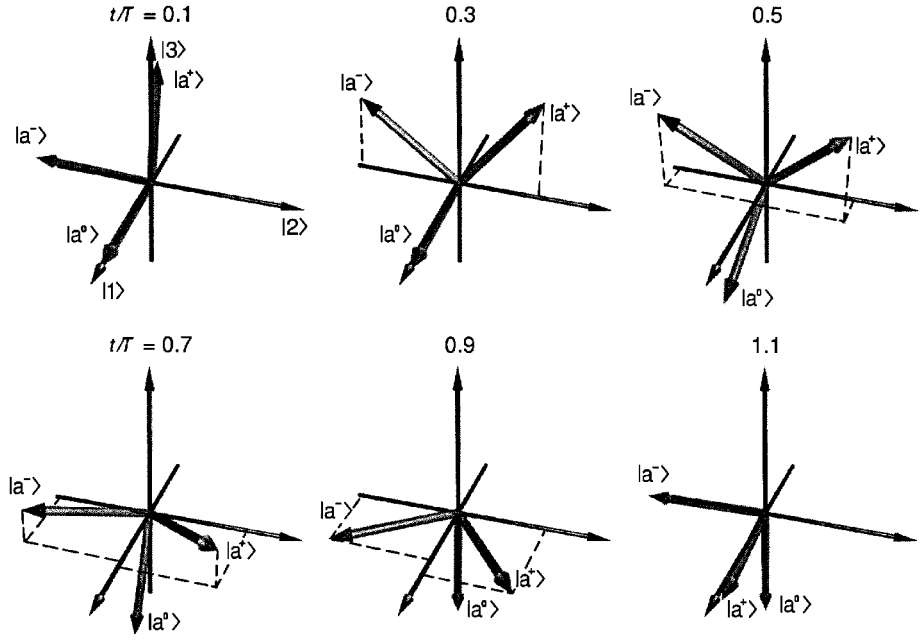

Fig. 6. As in Fig. 4, but for two-photon resonance with negative pump detuning ($\Delta_p = -0 \cdot 1\Omega_0$).

initial state $|\mathbf{1}\rangle$. As the pump pulse arrives, Θ starts to increase. After some time, the Stokes pulse reaches its maximum intensity. The system at this time is shown in the third panels of Figs 4–6 ($t/T = 0{\cdot}5$). Subsequently, the Stokes pulse starts to decrease in intensity while the pump-pulse intensity rises to its maximum value at $t/T = 0{\cdot}7$. The final part of the pulse sequence starts after the Stokes pulse has died away. This means that Θ has increased to $\pi/2$, so that $|\mathbf{a}^0\rangle$ lies along the desired final state $|\mathbf{3}\rangle$, as shown in the last panels. If adiabatic following has occurred, then the system will have followed $|\mathbf{a}^0\rangle$, moving smoothly from state $|\mathbf{1}\rangle$ to state $|\mathbf{3}\rangle$.

The value of ϕ during the pulse sequence depends on the detuning Δ_p, according to equation (15). If Δ_p is zero, then ϕ is $\pi/4$ at all times, as shown in Fig 4. With nonzero pump detuning, ϕ varies during the pulse sequence. For positive Δ_p, ϕ starts at zero and rapidly increases toward $\pi/4$ in the early part of the pulse sequence. During this time, Θ remains at zero (first panel of Fig. 5). In the middle part of the pulse sequence, ϕ changes little as Θ moves from zero to $\pi/2$. After the Stokes pulse has died away, ϕ returns to zero. Complementary behaviour occurs when Δ_p is negative: ϕ starts and finishes at $\pi/2$ and has values a little greater than $\pi/4$ in the middle part of the pulse sequence, as indicated in Fig. 6.

This motion of the triad for a system on two-photon resonance can be described as a rotation about the $|\mathbf{2}\rangle$ direction (the variation of Θ) combined with, if Δ_p is non zero, and a rotation about the instantaneous $|\mathbf{a}^0\rangle$ direction (the ϕ variation). At no time during the pulse sequence does $|\mathbf{a}^0\rangle$ contain any component of the intermediate state $|\mathbf{2}\rangle$, regardless of the value of Δ_p. In other words, Φ is zero at all times on two-photon resonance.

Off-resonance Systems

The three cases of two-photon resonance are the only situations in which the mixing angle Φ is always zero. It is clear from the rotation picture that this is the cause of a_2^0 always being zero. In this subsection, we examine the evolution of systems in which the unperturbed states $|\mathbf{1}\rangle$, $|\mathbf{2}\rangle$ and $|\mathbf{3}\rangle$ are all non degenerate; that is, $\Delta_\mathrm{p} \neq \Delta_3$ and neither is zero. There are six such generic cases, defined by the relative ordering of Δ_p, Δ_3 and zero. The three cases with $\Delta_\mathrm{p} > 0$ are treated here. The relationship between these and the cases with $\Delta_\mathrm{p} < 0$ is analogous to that between the cases in Figs 5 and 6.

Fig. 7 shows a case in which Δ_p and Δ_3 are opposite in sign. The corresponding eigenvector plot is Fig. 3*k*. In this situation, $|\mathbf{a}^0\rangle$ coincides with $|\mathbf{1}\rangle$ early in the pulse sequence and evolves toward $|\mathbf{3}\rangle$, like in the case of two-photon resonance. Indeed, all but the last panel of Fig. 7 are very similar to the corresponding panels in Fig. 5. However, as the Stokes pulse dies away, there is a sudden realignment so that $|\mathbf{a}^0\rangle$ returns to $|\mathbf{1}\rangle$ at the end of the pulse sequence. If adiabatic following were to occur, there would be no change of state.

The realignment occurs at the avoided crossing between ω^0 and ω^- shown in Fig. 3*k*. When eigenvalues change rapidly, as near an avoided crossing, the possibility of diabatic transitions is high. The triad-orientation plot clearly suggests that the state vector of the system is likely to retain its direction during the eigenvectors' sudden motion, so that, in the case shown in Fig. 7, the system will probably move from state $|\mathbf{a}^0\rangle$ to state $|\mathbf{a}^-\rangle$. This state then evolves to state $|\mathbf{3}\rangle$ as the pulse sequence ends, so effecting the desired transfer of population.

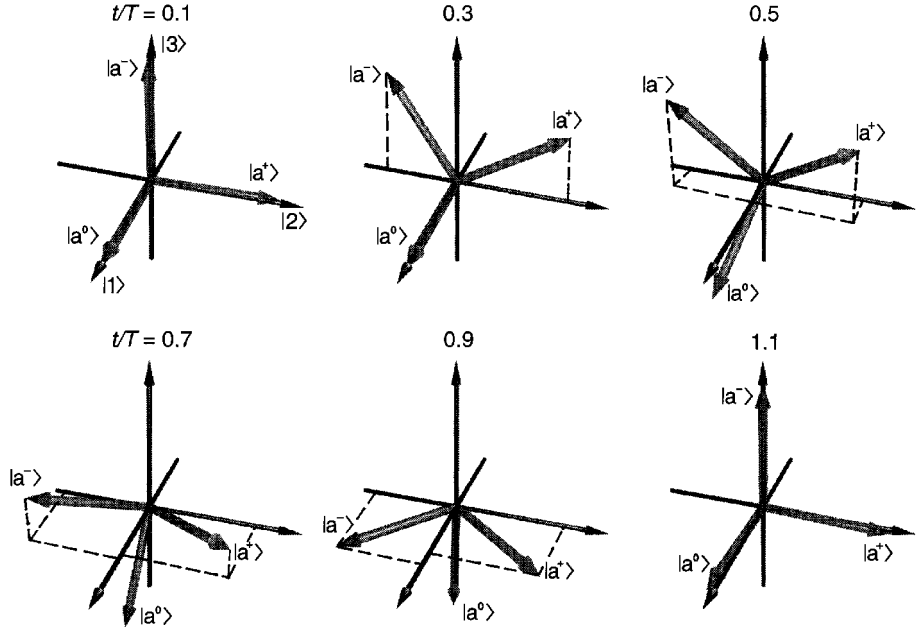

Fig. 7. As in Fig. 4, but for the off-resonance case with Δ_p opposite in sign to Δ_3 ($\Delta_p = 0{\cdot}1\Omega_0$, $\Delta_3 = -0{\cdot}1\Omega_0$).

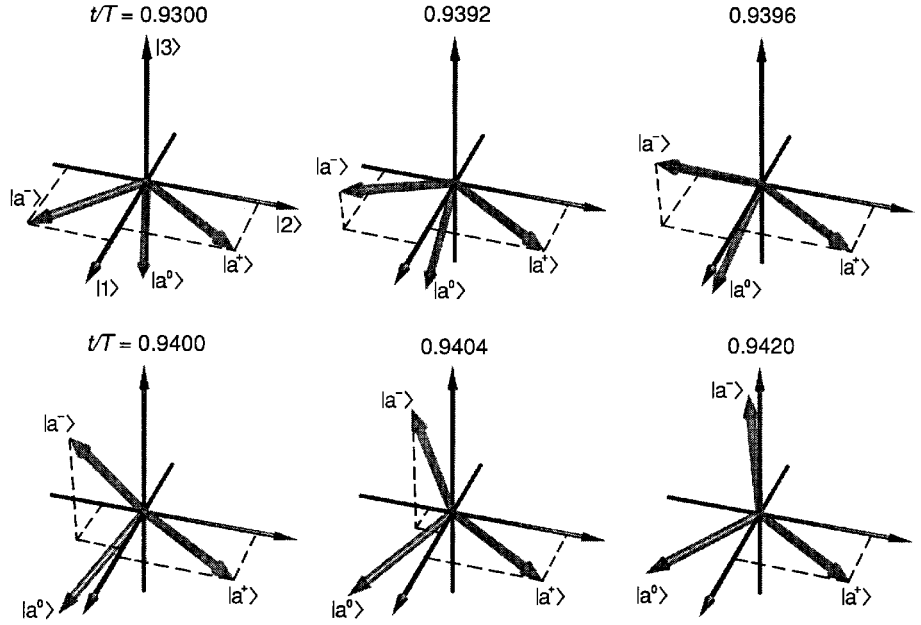

Fig. 8. As in Fig. 7, but a detail of the sudden realignment occurring late in the pulse sequence. The values of Δ_p and Δ_3 are the same as in Fig. 7. Note that the time intervals between panels are not equal.

The rapidity of the motion occurring between the last two panels of Fig. 7 is illustrated in Fig. 8, which shows views during the relevant period of time. For these parameter values, the angle Φ covers almost half of its entire range within a time of about $0{\cdot}004T$. The other two mixing angles also undergo large changes of value. It is interesting that, notwithstanding the magnitude of the changes in mixing angles, the eigenvector $|\mathbf{a}^+\rangle$ changes little during the realignment. As Fig. 8 illustrates, the motion is chiefly one of rotation about the direction of $|\mathbf{a}^+\rangle$.

During the realignment, rates of change of all mixing angles briefly exceed 500 rad per dimensionless time unit. This is over one hundred times greater than values typical away from the avoided crossing. It is unlikely that the system would adiabatically follow such rapid motion of the eigenvectors. Experimental studies support this view. Gaubatz *et al.* (1990), in a study of STIRAP in Na_2 molecules, list (their Table III) values of the range of two-photon detunings over which the efficiency of population transfer exceeds 50% of the maximum observed efficiency. That range varied from $0{\cdot}32\Omega_0$ when $\Delta_\mathrm{p} = 0$, down to $0{\cdot}09\Omega_0$ at $\Delta_\mathrm{p} = 10\Omega_0$, although the maximum transfer efficiency observed with the latter value of Δ_p was about 10%. Thus, detunings of the order of those used in Figs 7 and 8 are small enough to allow some significant population transfer.

Figs 9 and 10 show the other two cases of off-resonant systems that are treated here. The corresponding eigenvector plots are Figs $3f$ and $3b$. The behaviour here contrasts markedly with that shown in Figs 4–7, in that $|\mathbf{a}^0\rangle$ does not coincide with state $|\mathbf{1}\rangle$ at the beginning of the pulse sequence. State $|\mathbf{1}\rangle$ initially corresponds to $|\mathbf{a}^-\rangle$ when both detunings are positive, the situations shown in Figs 9 and 10, and with $|\mathbf{a}^+\rangle$ when both are negative. If the system follows these dressed states adiabatically, then it returns to state $|1\rangle$ at the end of the pulse sequence. In all of these cases, however, there is a rapid realignment of the dressed states soon after the pump pulse arrives, leading to the possibility of the system making a transition to state $|\mathbf{a}^0\rangle$. This realignment corresponds to the sharp avoided crossings in Figs $3f$ and $3b$. In cases where $0 > |\Delta_3| > |\Delta_\mathrm{p}|$ (Figs $3f$, 9), this would lead to the desired transfer of population; for $|\mathbf{a}^0\rangle$ evolves to $|\mathbf{3}\rangle$ at the end of the pulse sequence.

The case shown in Fig. 10, in which Δ_p lies between zero and Δ_3, is clearly less favourable for transfer than any of the cases so far discussed. In these situations, $|\mathbf{a}^0\rangle$ evolves not to $|\mathbf{3}\rangle$ but to $|\mathbf{2}\rangle$ as the pulse sequence passes. To obtain the desired population transfer, the system must make a second diabatic transition. The eigenvalue plot, Fig. $3b$, shows a second avoided crossing occurring somewhat after midway through the pulse sequence, but this is clearly much less sharp then the first avoided crossing. Thus, conditions are much less favourable for the second diabatic transition than for the first.

Pump and Stokes Resonance

Fig. 11 illustrates pump and Fig. 12 Stokes resonance. The corresponding eigenvector plots are Figs $3d$ and $3e$ respectively. In both cases, there is a two-fold degeneracy before and after the pulse sequence and one sharp avoided crossing.

In the case of pump resonance (Fig. 11), $|\mathbf{a}^0\rangle$ is aligned with $|\mathbf{1}\rangle$ at the beginning of the pulse sequence, and evolves toward $|\mathbf{3}\rangle$ as the sequence progresses.

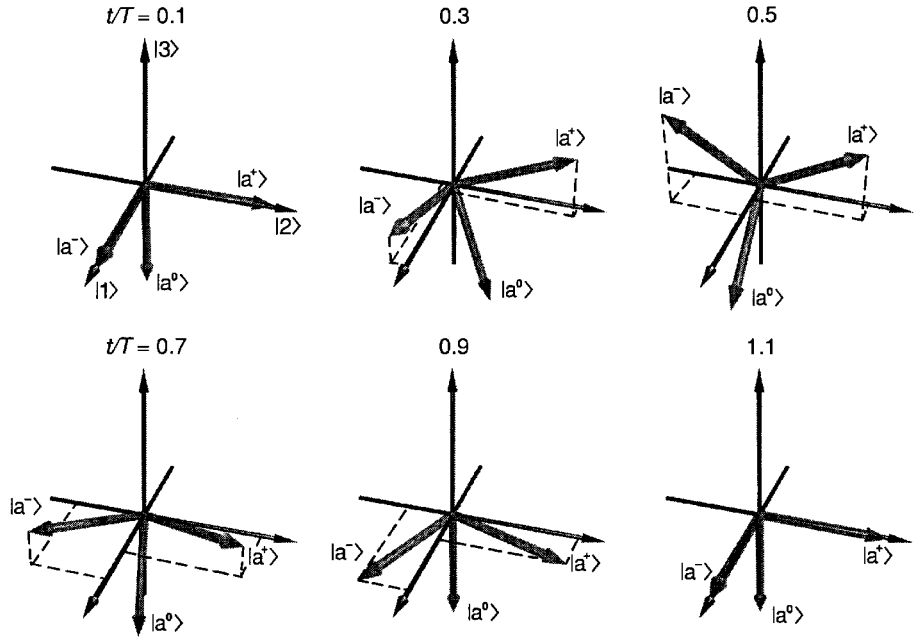

Fig. 9. As in Fig. 4, but for the off-resonance case with Δ_3 intermediate between zero and Δ_p ($\Delta_p = 0{\cdot}5\Omega_0$, $\Delta_3 = 0{\cdot}1\Omega_0$). Eigenstate $|\mathbf{a}^0\rangle$ is not the state vector of the system early in the pulse sequence.

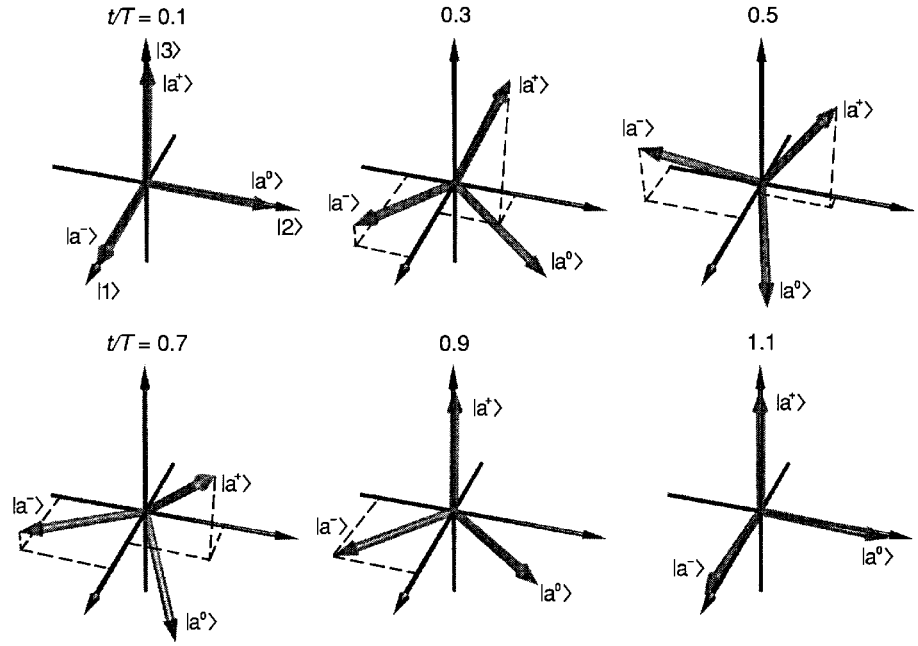

Fig. 10. As in Fig. 9, but for the off-resonance case with Δ_p intermediate between zero and Δ_3 ($\Delta_p = 0{\cdot}1\Omega_0$, $\Delta_3 = 0{\cdot}5\Omega_0$).

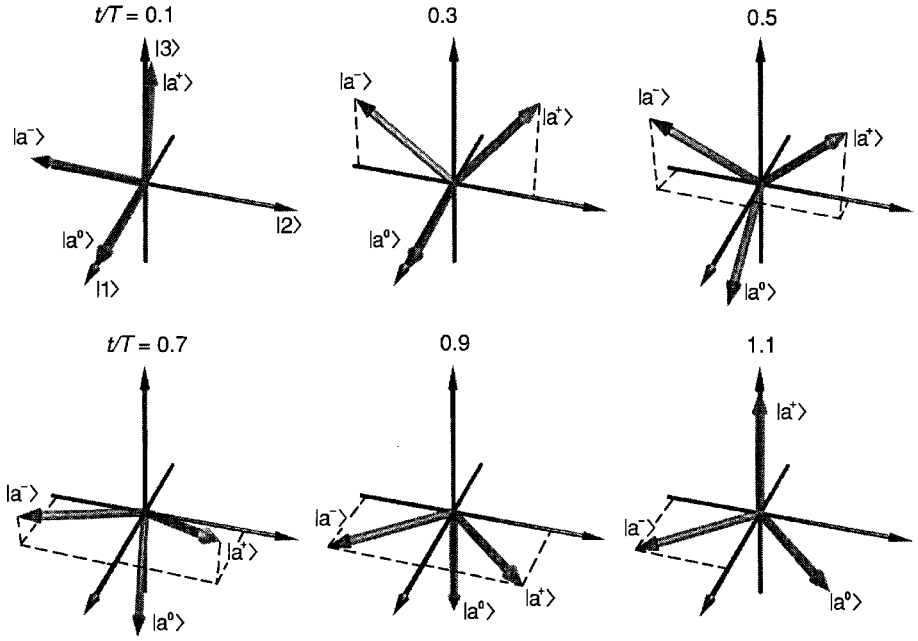

Fig. 11. As in Fig. 4, but for pump resonance ($\Delta_p = 0$, $\Delta_3 = 0 \cdot 1\Omega_0$). In this case, eigenstate $|\mathbf{a}^0\rangle$ is probably not the state vector of the system at the end of the pulse sequence.

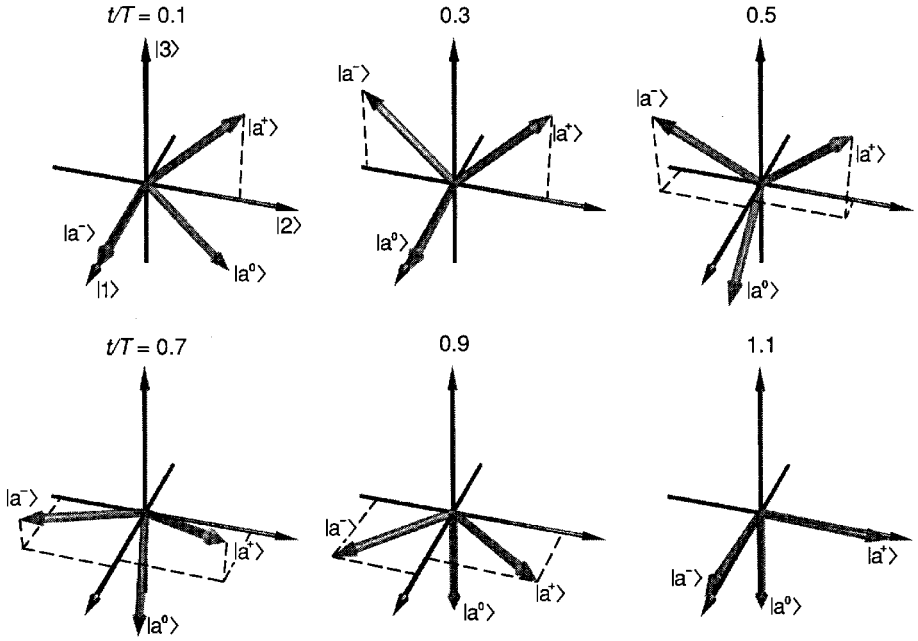

Fig. 12. As in Fig. 4, but for Stokes resonance ($\Delta_p = 0 \cdot 1\Omega_0$, $\Delta_3 = 0$). Here, the system starts in eigenstate $|\mathbf{a}^-\rangle$ but probably makes a diabatic transition to state $|\mathbf{a}^0\rangle$ early in the pulse sequence.

For the parameter values used in Fig. 11, the avoided crossings are even sharper than in the case shown in Fig. 8, with mixing-angle rates of change an order of magnitude larger during the realignment. Thus, there is likely to be a diabatic transition from $|\mathbf{a}^0\rangle$ to $|\mathbf{a}^+\rangle$ (to $|\mathbf{a}^-\rangle$ when Δ_3 is negative) leading to the desired population transfer.

The case of Stokes-beam resonance shown in Figs 12 and 3*e* is similar. Here, the system starts in $|\mathbf{a}^-\rangle$, makes a diabatic transition to $|\mathbf{a}^0\rangle$ early in the pulse sequence and then evolves adiabatically to $|\mathbf{3}\rangle$.

Summary

The above discussion suggests that adiabaticity is not as crucial a requirement for efficient population transfer as has been previously supposed. Indeed, it is shown in Section 2*b* that truly adiabatic population transfer requires *exact* two-photon resonance. Even the slightest detuning from resonance, as is inevitable in an experiment, will cause an avoided crossing with an accompanying rapid realignment of the eigenvectors. The present section demonstrates that this does not matter if the detuning is a small fraction of the peak Rabi frequency; for then a diabatic transfer will occur at the avoided crossing, resulting in the desired population transfer.

Of the cases considered in this section, one is clearly less favourable for population transfer than the rest. This is the case shown in Figs 10 and 3*b*, which requires two diabatic transitions to achieve the desired transfer of population; all other cases require at most one. In practical terms, this means that one should avoid situations in which the pump detuning Δ_p is of the same sign as and smaller in magnitude than the two-photon detuning Δ_3. For efficient transfer, the detunings should be as small as possible, with Δ_p not lying between zero and Δ_3.

(3d) Dark States

On two-photon resonance, the dressed state $|\mathbf{a}^0\rangle$ has zero projection on $|\mathbf{2}\rangle$ at all times. This is an important feature of STIRAP. Equation (25) in Appendix C shows that an eigenvector has zero projection on $|\mathbf{2}\rangle$ when its eigenvalue equals $2\Delta_3$. This occurs for $|\mathbf{a}^0\rangle$ at all times on two-photon resonance; for then ω^0 and Δ_3 are both zero throughout the pulse sequence. Fig. 3 shows that it does not happen in general. Indeed, $\omega = 2\Delta_3$ is consistent with the eigenvalue equation (equation 3) only if either $\Delta_3 = 0$ or $\Omega_\mathrm{s} = 0$, as substitution shows.

Although the component a_2^0 of state $|\mathbf{2}\rangle$ in $|\mathbf{a}^0\rangle$ is not zero off two-photon resonance, its value is small if the detunings are small. For example, in the case shown in Fig. 7, a_2^0 is initially zero and rises to about $0{\cdot}086$ in the middle of the pulse sequence. It then declines as the system approaches the avoided crossing with state $|\mathbf{a}^-\rangle$. The behaviour of a_2^0 and a_2^- in the region of the avoided crossing is shown in Fig. 13*a*. Each component is substantial for a brief period. We define a_2 as the component of $|\mathbf{2}\rangle$ in the state vector occupied by the system; a_2 is a time-varying linear combination of a_2^0 and a_2^-. Its maximum value depends on when the diabatic transition occurs, but cannot be less than the value at which the curves in Fig. 13*a* cross. This is about $0{\cdot}40$. Whether this and the nonzero value of a_2^0 earlier in the pulse sequence cause serious loss of population depends on the lifetime of state $|\mathbf{2}\rangle$ compared with the duration of the laser pulses.

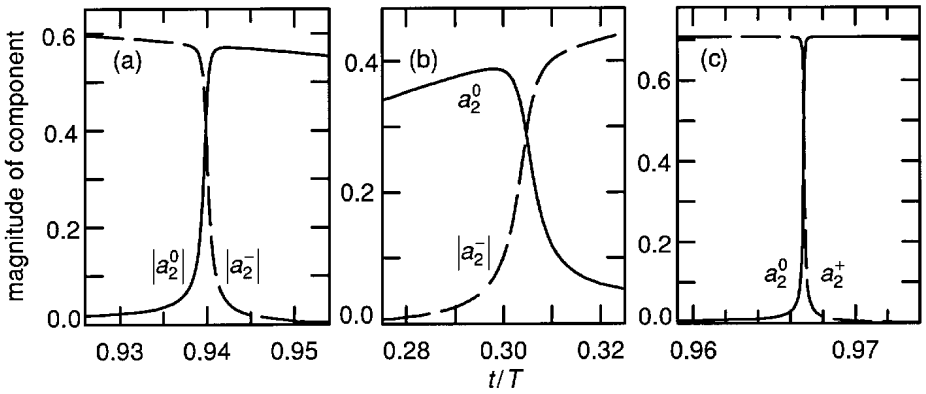

Fig. 13. Magnitudes $|a_2^i|$ of the $|2\rangle$-component of eigenstates involved in an avoided crossing in the region of that crossing for *(a)* $\Delta_\mathrm{p} = 0{\cdot}1\Omega_0$ and $\Delta_3 = -0{\cdot}1\Omega_0$, *(b)* $\Delta_\mathrm{p} = 0{\cdot}5\Omega_0$ and $\Delta_3 = 0{\cdot}1\Omega_0$, and *(c)* $\Delta_\mathrm{p} = 0$ and $\Delta_3 = 0{\cdot}1\Omega_0$.

Figs 13*b* and 13*c* show components of $|\mathbf{2}\rangle$ in the regions of the avoided crossings for the cases of $0 > |\Delta_3| > |\Delta_\mathrm{p}|$ (Figs 3*f* and 9) and pump resonance (Figs 3*d* and 11). The behaviour for Stokes resonance is similar to that shown in Fig. 13*c*. In each case, the value of a_2^0 is small away from the avoided crossing. The curves cross at a value of $0{\cdot}28$ in Fig. 13*b* and $0{\cdot}45$ in Fig. 13*c*. Thus, the off-resonant case of Fig. 13*b* has the least lower bound on a_2. However, the important quantity is not the maximum value of a_2, but rather its integral over the pulse sequence. On this view, Fig. 13*c* represents the most favourable of the situations shown in Fig. 13, because the crossing is comparatively abrupt. This emphasises once again the importance of minimising detuning.

4. Summary

The general problem of coherent adiabatic population transfer among three states has been solved algebraically. The resulting expressions encompass all situations of resonance or the lack thereof. These expressions are applied to the process of stimulated Raman scattering with adiabatic passage (STIRAP) in order to explore the sensitivity to two-photon resonance and to examine the relative importance of adiabatic evolution and diabatic transitions. We emphasise three basic points.

First, there is no adiabatic connection between the initial state $|\mathbf{1}\rangle$ and the final state $|\mathbf{3}\rangle$ unless one has exact two-photon resonance. This may seem central, but its importance is diminished by the second point: the importance of diabatic transitions between dressed states. When detunings are small, diabatic transitions are efficient in ensuring that the desired population transfer occurs. Thirdly, all eigenstates have non zero components of the intermediate state $|\mathbf{2}\rangle$ off two-photon resonance. This means that both population and coherence can be lost. However, if detunings are small, the rate of loss may be low enough to be tolerable.

Acknowledgments

We thank J. Junker and S. Steuerwald for their considerable assistance and effort in the preparation of Figs 4–12. M.P.F. warmly thanks members of the Fachbereich Physik der Universität Kaiserslautern for their hospitality during his period of study leave. This work was supported by the Deutsche Forschungsgemeinschaft under contract Be 623/21, by the Universität Kaiserslautern Graduierten Kolleg 'Laser und Teilchen Spektroskopie' and by a NATO Collaborative Research Grant. K.B. acknowledges partial support of this work by the network 'Laser controlled dynamics of molecular processes and applications' of the European Union (contract No. ERB-CHR-XCT-64–0603). The work of B.W.S. is supported in part under the auspices of the U.S. Department of Energy at Lawrence Livermore National Laboratory under contract W-7405-Eng-48.

References

Abramowitz, M., and Stegun, I. A. (1973). 'Handbook of Mathematical Functions', 9th Printing, p. 17 (Dover: New York).
Adams, A. G., Gough, T. T., Isenor, N. R., and Scoles, G. (1985). *Phys. Rev.* A **29**, 1451.
Agarwal, G. S., and Jha, S. S. (1979). *J. Phys.* B **12**, 2655.
Alzetta, G., Moi, L., and Orriols, G. (1979). *Nuovo Cim.* **52 B**, 209.
Arimondo, E., and Orriols, G. (1976). *Lett. Nuovo Cim.* **17**, 333.
Avrillier, S., Raimond, J. M., Borde, Ch. J., Bassi, D., and Scoles, G. (1981). *Opt. Commun.* **39**, 311.
Bergmann, K., Martin, J., and Shore, B. W. (1995). *In* 'Molecular Dynamics and Spectroscopy by Stimulated Emission Pumping' (Eds H. L. Dai and R. W. Field), p. 315 (World Scientific: Singapore).
Broers, B., van Linden van den Heuvell, H. B., and Noordam, L. D. (1992). *Phys. Rev. Lett.* **69**, 2062.
Carroll, C. E. (1989). *Phys. Rev.* A **39**, 2243.
Carroll, C. E., and Hioe, F. T. (1986*a*). *J. Phys.* A **19**, 2061.
Carroll, C. E., and Hioe, F. T. (1986*b*). *J. Phys.* A **19**, 3579.
Carroll, C. E., and Hioe, F. T. (1987*a*). *Phys. Rev.* A **36**, 724.
Carroll, C. E., and Hioe, F. T. (1987*b*). *Phys. Rev.* A **36**, 3000.
Carroll, C. E., and Hioe, F. T. (1988*a*). *J. Math. Phys.* **29**, 487.
Carroll, C. E., and Hioe, F. T. (1988*b*). *J. Opt. Soc. Am.* B **5**, 1335.
Carroll, C. E., and Hioe, F. T. (1989). *J. Phys.* B **22**, 2633.
Carroll, C. E., and Hioe, F. T. (1992). *Phys. Rev. Lett.* **68**, 3523.
Carroll, C. E., and Hioe, F. T. (1993). *Phys. Rev.* A **47**, 571.
Carroll, C. E., and Hioe, F. T. (1995). *Phys. Lett.* A **199**, 145.
Chang, C. S., and Schlier, R. (1980). *Phys. Rev.* A **21**, 872.
Coulston, G. W., and Bergmann, K. (1992). *J. Chem. Phys.* **96**, 3467.
Dam, N., Oudejans, L., and Reuss, J. (1990). *Chem. Phys.* **140**, 217.
Danileiko, M. V., Romanenko, V. I., and Yatsenko, L. P. (1994). *Opt. Commun.* **109**, 462.
Dittmann, P., Pesl, F. P., Martin, J., Coulston, G. W., He, G.-Z., and Bergmann, K. (1992). *J. Chem. Phys.* **97**, 9472.
Gaubatz, U., Rudecki, P., Schiemann, S., and Bergmann, K. (1990). *J. Chem. Phys.* **92**, 5363.
Goldner, L. S., Gerz, C., Spreeuw, R. J. C., Rolston, S. L., Westbrook, C. I., Phillips, W. D., Marte, P., and Zoller, P. (1994). *Phys. Rev. Lett.* **72**, 997.
Halfmann, T., and Bergmann, K. (1996). *J. Chem. Phys.* **104**, 7068.
Hamadani, S. M., Mattick, A. T., Kurnit, N. A., and Javan, A. (1975). *Appl. Phys. Lett.* **27**, 21.
He, G.-Z., Kuhn, A., Schiemann, S., and Bergmann, K. (1990). *J. Opt. Soc. Am.* B **7**, 1960.
Hioe, F. T. (1987). *J. Opt. Soc. Am.* B **4**, 1327.
Kancheva, L., Pushkarov, D., and Rashev, S. (1981). *J. Phys.* B **14**, 573.
Kasevich, M., and Chu, S. (1991). *Phys. Rev. Lett.* **67**, 181.

Kasevich, M., and Chu, S. (1992). *Phys. Rev. Lett.* **69**, 1741.
Kasevich, M., Weiss, D. S., Riis, E., Moler, K., Kasapi, S., and Chu, S. (1991). *Phys. Rev. Lett.* **66**, 2297.
Kuhn, A., Coulston, G. W., He, G.-Z., Schiemann, S., Bergmann, K., and Warren, W. S. (1992). *J. Chem. Phys.* **96**, 4215.
Kuklinski, J. R., Gaubatz, U., Hioe, F. T., and Bergmann, K. (1989). *Phys. Rev.* A **40**, 6741.
Külz, M., Keil, M., Kortyna, A., Schellhaass, B., Hauch, J., Bergmann, K., Weyh, D., and Meyer, W. (1996). *Phys. Rev.* A **53**, 3324.
Kuz'min, M. V. (1981). *Kvant. Elektron. (Moscow)* **8**, 20 [English Trans: *Sov. J. Quant. Electron.* **11** (1981) 9].
Kuz'min, M. V., and Sazonov, V. N. (1980). *Zh. Eksp. Teor. Fiz.* **79**, 1759 [English Trans: *Sov. Phys. JETP* **52** (1980) 889].
Lawall, J., and Prentiss, M. (1994). *Phys. Rev. Lett.* **72**, 993.
Manka, A. S., Doss, H. M., Narducci, L. M., Ru, P., and Oppo, G.-L. (1991). *Phys. Rev.* A **43**, 3748.
Marte, P., Zoller, P., and Hall, J. L. (1991). *Phys. Rev.* A **44**, 4118.
Martin, J. (1995). Ph.D. Thesis, Universität Kaiserslautern.
Martin, J., Shore, B. W., and Bergmann, K. (1995). *Phys. Rev.* A **52**, 583.
Martin, J., Shore, B. W., and Bergmann, K. (1996). *Phys. Rev.* A **54**, 1566.
Messiah, A. (1962). 'Quantum Mechanics', Vol. 2, p. 525 (North Holland: Amsterdam).
Nakajima, T., Elk, M., Zhang, J., and Lambropoulos, P. (1994). *Phys. Rev.* **50**, 913.
Narducci, L. M., Scully, M. O., Oppo, G.-L., Ru, P., and Tredicce, J. R. (1990). *Phys. Rev.* A **42**, 1630.
Oreg, J., Bergmann, K., Shore, B. W., and Rosenwaks, S. (1992). *Phys. Rev.* A **45**, 4888.
Oreg, J., Hazak, G., and Eberly, J. H. (1985). *Phys. Rev.* A **32**, 2776.
Oreg, J., Hioe, F. T., and Eberly, J. H. (1984). *Phys. Rev.* A **29**, 690.
Orriols, G. (1979). *Nuovo Cim.* **53** B, 1.
Radmore, P. M. (1982). *Phys. Rev.* A **26**, 2252.
Radmore, P. M., and Knight, P. L. (1982). *J. Phys.* B **15**, 561.
Rubahn, H.-G., Konz, E., Schiemann, S., and Bergmann, K. (1991). *Z. Phys.* D **22**, 401.
Sarkisyan, M. A., and Ter-Mikaelyan, M. L. (1978). *Izv. Akad. Nauk SSSR*, Ser. Fiz. **42**, 2574.
Schiemann, S., Kuhn, A., Steuerwald S., and Bergmann, K. (1993). *Phys. Rev. Lett.* **71**, 3637.
Senitzky, I. R. (1982). *Phys. Rev. Lett.* **49**, 1636.
Shore, B. W. (1990). 'The Theory of Coherent Atomic Excitation' (Wiley: New York).
Shore, B. W., Bergmann, K., Oreg, J., and Rosenwaks, S. (1991). *Phys. Rev.* A **44**, 7442.
Shore, B. W., Bergmann, K., Kuhn, A., Schiemann, S., Oreg, J., and Eberley, J. H. (1992). *Phys. Rev.* A **45**, 5297.
Shore, B. W., Martin, J., Fewell, M. P., and Bergmann, K. (1995). *Phys. Rev.* A **52**, 566.
Süssmann, R., Neuhauser, R., and Neusser, H. F. (1994). *J. Chem. Phys.* **100**, 4784.
Wilson, R. J., and Hahn, E. L. (1982). *Phys. Rev.* A **26**, 3404.
Zare, R. N. (1988). 'Angular Momentum', pp. 77–81 (Wiley: New York).

Appendix A: Labelling the Eigenvalues

The labels of the eigenvalues used in this paper conform with those used by Kuklinski *et al.* (1989) and Gaubatz *et al.* (1990) in the case of two-photon resonance. Expressions for the eigenvalues on two-photon resonance (equations 16) are obtained much more easily by direct solution of the eigenvalue equation (equation 3) than by setting $\Delta_3 = 0$ in equations (4–6). Indeed, Appendix B shows that reduction of equations (4–6) to the two-photon case causes all information on labelling to be lost.

Verification that the labelling of the roots in equations (4) corresponds to that in equations (16) is easily done by examining the case of one-photon resonance, for which $\Delta_p = \Delta_3 = 0$. Substitution of this in equations (5) and (6) gives

$\zeta = 3\pi/2$, since the value of the inverse cosine function is taken to lie in the range $[0, \pi]$. This gives the desired verification, by direct substitution in equations (4).

Appendix B: Reduction of the General Eigenvalue Expressions to the Case of Two-photon Resonance

In the case of two-photon resonance ($\Delta_3 = 0$), equation (6) gives

$$\zeta = 2\pi - \arccos \frac{\Delta_\mathrm{p}(9\Omega_\mathrm{p}^2 + 9\Omega_\mathrm{s}^2 + 8\Delta_\mathrm{p}^2)}{(3\Omega_\mathrm{p}^2 + 3\Omega_\mathrm{s}^2 + 4\Delta_\mathrm{p}^2)^{\frac{3}{2}}} \,. \tag{21}$$

To show that equations (4) do indeed reproduce equations (16) for this value of ζ, it is necessary to obtain an expression for $\zeta/3$. In principle, this is contained in the trigonometric identity

$$4\cos^3(\zeta/3) - 3\cos(\zeta/3) = \cos\zeta \,, \tag{22}$$

an equation which cannot, in general, be solved algebraically. However, it is straightforward to verify that

$$\cos(\zeta/3) = -\Delta_\mathrm{p}(3\Omega_\mathrm{p}^2 + 3\Omega_\mathrm{s}^2 + 4\Delta_\mathrm{p}^2)^{-1/2} \tag{23}$$

satisfies equation (22) when ζ is given by equation (21).

Application of equation (23) is not as simple as it may appear; for, if ζ is a solution to equation (22), then so is $2\pi \pm \zeta$. That is, the right-hand side of equation (23) can refer to the cosine of any of the three angles required. Indeed, these are simply the three roots of equation (22). Thus, use of equation (22) causes all information on the labelling of the eigenvectors to be lost. Equations (7) provide the way forward. Clearly, the right-hand side of equation (23) is bounded by $\pm\frac{1}{2}$, approaching these limits when $\Delta_\mathrm{p}^2 \gg \Omega_\mathrm{p}^2 + \Omega_\mathrm{s}^2$. Thus, equation (23) can be used directly in equations (4), and a little algebraic manipulation shows that this reduces them to equations (16).

Appendix C: Values of the Mixing Angles Θ and Φ

Equations (11) define a parametrisation of $|\mathbf{a}^i\rangle$ using mixing angles. Expressions for the mixing angles in terms of the detunings and Rabi frequencies are obtained by matching the components a_k^i of an eigenvector, defined by

$$|\mathbf{a}^i\rangle = a_1^i|\mathbf{1}\rangle + a_2^i|\mathbf{2}\rangle + a_3^i|\mathbf{3}\rangle \;\text{ for }\; i = -, 0, + \,, \tag{24}$$

with solutions to the eigenvector equations:

$$\begin{aligned} -\omega^i a_1^i + \Omega_\mathrm{p} a_2^i &= 0, \\ \Omega_\mathrm{p} a_1^i + (2\Delta_\mathrm{p} - \omega^i) a_2^i + \Omega_\mathrm{s} a_3^i &= 0 \,, \\ \Omega_\mathrm{s} a_2^i + (2\Delta_3 - \omega^i) a_3^i &= 0 \,. \end{aligned} \tag{25}$$

Only two of these three equations are linearly independent. In some situations, the choice of equations matters. For example, on two-photon resonance both Δ_3 and ω^0 are zero, and so, when calculating the components of $|\mathbf{a}^0\rangle$, the first and last lines of equation (20) are identical. No pair of equations (25) works in all situations.

It may seem that mixing angle Φ is the most straightforward to obtain, since equation (11) shows that $\tan\Phi$ is given by the ratio $-a_2^0/a_3^0$. However, it is equally clear that this cannot work when Θ is zero; for then equation (11) contains no information on Φ. It is necessary to calculate Θ first.

Equation (11) gives

$$\tan\Theta = \frac{[(a_2^0)^2 + (a_3^0)^2]^{\frac{1}{2}}}{|a_1^0|}\,. \tag{26}$$

Ratios of the components a_k^0 can be determined from the second line of equation (25) and one other. We use the last line of equation (25) except when $\Omega_\mathrm{s} = 0$ and either $\Delta_3 = \Delta_\mathrm{p}$ or $\Delta_3 = 0$. In these cases, $\omega^0 = 2\Delta_3$, and so the last line of equation (25) contains no information about the components of $|\mathbf{a}^0\rangle$. Inspection shows that $\Theta = \pi/2$ in both situations. We thus obtain equation (14). It can be seen that the argument of the arctan function in equation (14) is strictly indeterminate when $\omega^0 = 2\Delta_3$ and $\Omega_\mathrm{s} = 0$.

Note that Θ cannot be zero unless a Rabi frequency is zero. This can be deduced from equations (25) and (11) in the following way. Equations (25) show that, if two components of an eigenvector are zero and both Ω_p and Ω_s are nonzero, then the third component of the eigenvector must also be zero. But this is a contradiction, since we require eigenvectors to be always normalisable. Thus, at most one component of any eigenvector can be zero when both Ω_p and Ω_s are nonzero. However, the first line of equation (11) shows that two components of $|\mathbf{a}^0\rangle$ are zero when Θ is zero. Thus, Θ cannot be zero when both Ω_p and Ω_s are nonzero. Of course, the manner in which the system evolves when one Rabi frequency is zero is crucial to STIRAP and so these cases require detailed consideration.

Having obtained Θ, Φ can be calculated. This is given by the ratio $-a_2^0/a_3^0$ unless Θ equals zero. In this case, Φ is indistinguishable from ϕ. Equations (11) show that the eigenvectors depend only on $\phi - \Phi$ when Θ equals zero. We choose to set Φ to zero in this situation, leading to equation (15).

If Φ is a solution of equation (15), then so is $\Phi + \pi$. Which of these is correct can be checked by examining the relative sign of a pair of eigenvector components, but the correct choice of a pair for this purpose depends on the value of ϕ. Thus, the question of the quadrant of Φ is deferred to Appendix E, after the calculation of ϕ. This calculation requires expressions for Φ, but these are insensitive to a difference of π.

Appendix D: Values of the Mixing Angle ϕ

There are many possible expressions for the angle ϕ. Any pair of the components of either $|\mathbf{a}^+\rangle$ or $|\mathbf{a}^-\rangle$ could be chosen, and, for each of these six choices, any pair of equations (25) could supply expressions for the ratio of components. However, each of these choices has special cases in which it fails. The general

rules applying to the identification of these cases are obtained from equations (11) and (25). As an example, consider the middle line of equation (11). When $\Theta = \pi/2$, this equation reads

$$|\mathbf{a}^+\rangle = \sin\phi|\mathbf{1}\rangle + \cos\Phi\cos\phi|\mathbf{2}\rangle + \sin\Phi\cos\phi|\mathbf{3}\rangle.$$

The ratio a_2^+/a_3^+ is now independent of ϕ, and so clearly cannot be used to obtain the value of ϕ. Considerations of this sort lead to the rules summarised in Table 3. Similar constraints apply in the choice of pairs of equations from equations (25) to obtain expressions for the component ratios. Taking equations (25) in conjunction with the eigenvalue equation (equation 3) gives the rules in Table 4.

Table 3. Constraints on the choice of component ratios for use in the calculation of ϕ arising from the form of equations (11)

If $\Theta = 0$:	Use a_2^+/a_3^+ or a_2^-/a_3^-
If $\Phi = 0$:	Do not use a_1^+/a_3^+ or a_1^-/a_3^-
If $\Phi = \pm\pi/2$:	Do not use a_1^+/a_2^+ or a_1^-/a_2^-
If $\Theta = \pi/2$:	Do not use a_2^+/a_3^+ or a_2^-/a_3^-

Table 4. Constraints on the choice of pairs of equations for obtaining expressions for component ratios

If $\Omega_\mathrm{p} = 0$:	Use second and third lines of equations (25) if $\omega^i = 0$, otherwise do not use this pair
If $\Omega_\mathrm{s} = 0$:	Use first and second lines of equations (25) if $\omega^i = 2\ \Delta_3$, otherwise do not use this pair
If $\Delta_3 = 0$:	Do not use first line of equation (25) together with last line

Use of the rules in Tables 3 and 4 ensures that the chosen eigenvector components are not both zero and that their ratio contains some dependence on ϕ. For the sake of numerical stability, it is desirable that both are not close to zero. Examination of all the special cases arising when one Rabi frequency is zero leads to the scheme set out in Table 1. The spline points are located arbitrarily at $\pi/20$ in the interests of numerical stability. The scheme given Table 1 is not unique; other choices of expressions are possible, some of which are as good. However, we doubt that fewer expressions could be employed without endangering numerical stability.

Appendix E: Range of the Mixing Angle Φ

The final step in the calculation of the mixing angles is the determination of the range of the angle Φ. The standard root of equation (15) lies in the range $[-\pi/2, \pi/2]$. Whether or not this is the correct solution can be determined by examining ratios of eigenvector projections. For example, inspection of equation (11) shows that, if $-\pi/2 < \Phi < \pi/2$, then the ratio a_3^0/a_1^0 is negative. An expression for this ratio can be obtained from equations (25); if it is found to be positive, then π must be added to Φ. Unfortunately, as in the computation of ϕ, complications arise in various special cases. For example, the ratio a_3^0/a_1^0

cannot contain the desired information if Θ equals either zero or $\pi/2$. Also, the rules in Table 4 must be followed in selecting the pair of equations (25) to use in obtaining the expression for the selected ratio. This must be done separately for various cases. We verify below that, when all of the special cases are examined, Φ always lies in the range $-\pi/2 \leq \Phi \leq \pi/2$ as stated in equation (13).

The Mixing Angle Θ neither Zero nor $\pi/2$

In this case, state $|\mathbf{a}^0\rangle$ has non zero projections on at least two of the unperturbed states. The cases of $\Phi = \pm\pi/2$ require no further examination, so it is convenient to consider the ratio a_3^0/a_1^0. Equation (11) gives

$$a_3^0/a_1^0 = -\cos\Phi\tan\Theta\,. \tag{28}$$

An independent expression for a_3^0/a_1^0 can be obtained from equations (25), observing the constraints in Table 4. Since Θ is neither zero nor $\pi/2$, $\Omega_\mathrm{p} \neq 0$, leading to the result

$$-\pi/2 \leq \Phi \leq \pi/2 \quad \text{if} \quad \begin{cases} 4\Delta_3(\Delta_3 - \Delta_\mathrm{p}) < \Omega_\mathrm{p}^2 & \text{if } \omega^0 = 2\Delta_3 \\ (\omega^0 - 2\Delta_\mathrm{p})(\omega^0 - 2\Delta_3) < \Omega_\mathrm{p}^2 & \text{otherwise}\,. \end{cases} \tag{29}$$

Manipulation of the eigenvalue equation shows that these conditions are always fulfilled when $\Omega_\mathrm{p} \neq 0$.

The Mixing Angle $\Theta = \pi/2$

Equation (28) is not useful in this case; information on the quadrant of Φ must be obtained from another dressed state. The second and third lines of equation (11) reduce to

$$a_2^+/a_1^+ = -\cos\Phi\cot\phi, \quad a_2^-/a_1^- = -\cos\Phi\tan\phi\,. \tag{30}$$

Using Table 4 to select the appropriate pairs from equations (25), we conclude that

$$-\pi/2 \leq \Phi \leq \pi/2 \quad \text{if} \quad \begin{cases} \omega^+ \geq 0, & \text{if } \Delta_\mathrm{p} \geq 0 \\ \omega^- < 0, & \text{otherwise.} \end{cases} \tag{31}$$

It is clear from the behaviour of the eigenvalues that the conditions of equation (31) are always fulfilled.

The Mixing Angle $\Theta = 0$

Equation (28) is again not useful. Here, $|\mathbf{a}^0\rangle$ equals $|1\rangle$ and $|\mathbf{a}^\pm\rangle$ are independent of $|1\rangle$. Thus our phase convention provides no information on the quadrant of Φ. We treat this case by examining the development of the dressed states under a STIRAP pulse sequence, requiring that, as the states $|\mathbf{a}^\pm\rangle$ gain projections on $|1\rangle$, no sudden change in the phases of $a_2^\pm$ and $a_3^\pm$ should occur. In all situations, this rule requires Φ to lie in the range $[-\pi/2, \pi/2]$ when $\Theta = 0$.

Manuscript received 26 June, accepted 15 November 1996